

DMD #23390

Title Page

L-Methionine-*dl*-sulfoxide metabolism and toxicity in freshly isolated mouse
hepatocytes: Gender differences and inhibition with aminooxyacetic acid

Joseph T. Dever and Adnan A. Elfarra

Department of Comparative Biosciences and Molecular and Environmental Toxicology

Center, University of Wisconsin-Madison, Madison, Wisconsin

DMD #23390

Running Title Page

Methionine sulfoxide metabolism and toxicity

Corresponding author: Dr. Adnan Elfarra, University of Wisconsin-Madison, School of
Veterinary Medicine, 2015 Linden Dr, Madison, WI 53706-1102

(608)262-6518 – office (608)263-3926 – fax elfarra@svm.vetmed.wisc.edu

Text pages: 28

Tables: 1

Figures: 8

References: 37

Words in abstract: 250

Words in introduction: 706

Words in discussion: 1184

Abbreviations

Abbreviations used are: MetO, L-methionine-*dl*-sulfoxide; Met-*d*-O, L-methionine-*d*-sulfoxide; Met-*l*-O, L-methionine-*l*-sulfoxide; Met, L-methionine; Msrs, Peptide methionine sulphoxide reductases; FMO, Flavin-containing monooxygenase; ROS, reactive oxygen species; AOAA, aminooxyacetic acid; TA, transamination; PhP, phenylpyruvate; GTK, glutamine transaminase K; TB, trypan blue; LDH, lactate dehydrogenase; DMEM, Dulbecco's modified Eagle's Medium; EDTA, ethylenediaminetetraacetic acid; SSA, 5-sulfosalicylic acid; GSH, glutathione; GSSG, glutathione disulfide; AUC, area under the curve; HPLC, high performance liquid chromatography

DMD #23390

Abstract

L-Methionine-*dl*-sulfoxide (MetO) is an L-methionine (Met) metabolite, but its role in Met metabolism and toxicity is not clear. In this study, MetO uptake, metabolism to Met, cytotoxicity, and GSH and GSSG status were characterized in freshly isolated mouse hepatocytes incubated at 37°C with 0-30 mM MetO for 0-5 h. In male hepatocytes, dose-dependent cytotoxicity concomitant with GSH depletion without GSSG formation occurred after exposure to 20 or 30 mM MetO, but not 10 mM MetO. Interestingly, female hepatocytes exposed to 30 mM MetO showed no cytotoxicity and exhibited increased intracellular GSH levels compared to control hepatocytes. Male hepatocytes had approximately 2-fold higher levels of intracellular Met-*d*-O or Met-*l*-O after MetO (30 mM) exposure for 0-1.5 h compared to female hepatocytes. In hepatocytes of both genders, Met-*l*-O was detected at nearly 5-fold higher levels than Met-*d*-O, and no significant increase in cellular Met levels was detected. Addition of aminooxyacetic acid (AOAA), an inhibitor of transamination reactions, to MetO-exposed male hepatocytes resulted in higher cellular Met-*d*-O and Met-*l*-O levels and decreased the cytotoxicity of MetO. Interestingly, exposure of control male hepatocytes to AOAA selectively increased cellular Met-*d*-O levels to levels similar to those observed after exposure to MetO (30mM). Analysis of MetO transamination activity by glutamine transaminase K in mouse liver cytosol revealed similar rates of MetO transamination in cytosol of both genders. Taken together, these results provide evidence for stereoselective oxidation of Met to Met-*d*-O under physiological conditions and suggest a major role for MetO transamination in MetO metabolism and toxicity.

DMD #23390

Introduction

L-Methionine-*dl*-sulfoxide (MetO) is an oxidative metabolite of the essential amino acid L-methionine (Met). MetO is present at low levels in healthy human plasma (Mashima et al., 2003) and at higher levels in humans with hypermethionemia (Perry et al., 1967; Gahl et al., 1988), a condition associated with hepatotoxicity and growth depression in humans and various animal models by mechanisms that have not been fully established (Shinozuka et al., 1971; Steele et al., 1978; Moss et al., 1999).

While the primary mechanism of *in vivo* MetO formation is not clear, chemical and enzymatic *S*-oxidation of Met have been characterized. Met *S*-oxidation by reactive oxygen species (ROS) such as peroxyxynitrite, hypochlorite, hydrogen peroxide, and singlet oxygen has been demonstrated *in vitro* under physiological conditions (Mashima et al., 2003) and has been implicated in the sulfoxidation of Met-residues in proteins (Stadtman et al., 2004; Sharov and Schoneich, 2000). Our laboratory has also characterized the *in vitro* enzymatic formation of MetO by mammalian flavin-containing monooxygenases (FMOs). Among the FMO isoforms examined (FMO1, FMO2, FMO3, and FMO5), FMO3, present in both male and female human liver microsomes (Ripp et al., 1999), *S*-oxidizes Met with the lowest K_m (6.5 mM with rabbit cDNA-expressed FMO3) and forms much higher levels of methionine-*d*-sulfoxide (Met-*d*-O) than methionine-*l*-sulfoxide (Met-*l*-O) (Duescher et al., 1994). FMO3 is also expressed in female mouse liver microsomes whereas male mouse liver microsomes do not express this enzyme (Ripp et al., 1999). An unidentified Met *S*-oxidase activity has, however, been detected in male mouse liver microsomes, and this activity also preferentially forms Met-*d*-O (Ripp et al., 1999). Interestingly, Met-*d*-O has been detected in the urine of a hypermethionemic

DMD #23390

human with Met adenosyltransferase deficiency (Gahl et al., 1988) and was also the primary MetO diastereomer detected in the liver and plasma of male and female mice given a single dose of Met (400 mg/kg) (Dever and Elfarra, 2006). It is not known if the detection of primarily Met-*d*-O in these studies resulted from stereoselective formation of Met-*d*-O from Met or stereoselective further metabolism of Met-*l*-O.

Knowledge of the metabolic fate of MetO is limited (Figure 1). MetO has been shown to be metabolically utilized by humans and animal models (Mashima et al., 2003; Stegink et al., 1986). It can also function as a partial nutritional replacement for Met in rats suggesting that MetO can be metabolically converted to Met (Miller et al., 1970; Anderson et al., 1976). Peptide methionine sulfoxide reductases (Msrs) catalyze the reduction of free or protein-bound MetO (Moskovitz et al, 2002) and may contribute to the *in vivo* conversion of MetO to Met. Alternatively, *N*-acetylation of MetO has been detected in rats dosed with high levels of MetO (Smith, 1972). MetO was also shown to be a substrate for glutamine transaminase *in vitro* (Cooper and Meister, 1972). These studies suggest several potential metabolic pathways for MetO, however, their relative contributions to MetO metabolism are not clear.

In summary, Met *S*-oxidation has been shown to be a significant Met metabolic pathway in hypermethionemic humans and mice, but the fate of MetO and its role in overall Met metabolism and toxicity are not known. Thus, the present studies were undertaken to characterize MetO cellular uptake, metabolism to Met, and toxicity in freshly isolated male and female mouse hepatocytes. Hepatocytes were chosen for these experiments since the liver is the primary organ involved in Met metabolism and is a target of Met toxicity. The toxicity of MetO was assessed by measuring cell viability via

DMD #23390

trypan blue (TB) exclusion and LDH leakage assays as well as cellular and medium GSH and GSSG status in male and female mouse hepatocytes exposed to increasing concentrations of MetO for 0-5 h. To assess cellular MetO uptake and its metabolism to Met at time points that preceded the toxicity, an HPLC method was developed to measure cellular Met-*d*-O, Met-*l*-O, and Met levels in MetO-exposed hepatocytes of both genders from 0 to 1.5 h. To examine the role of MetO transamination (TA) in MetO metabolism and hepatotoxicity, the effects of the transaminase inhibitor aminoxyacetic acid (AOAA) (Mitchell and Benevenga, 1978) on MetO metabolism and toxicity in male hepatocytes were also determined. Additionally, MetO transamination activity by glutamine transaminase K (GTK) was measured in mouse liver cytosol of both genders.

DMD #23390

Materials and Methods

Chemicals. Trypsin inhibitor (type II-O), collagenase (Type IV), MetO, Met, AOAA, GSH, GSSG, GSH reductase, 5,5'-dithio-bis(2-nitrobenzoic acid, pyruvate, NADH, NADPH, 2-vinylpyridine, 5-sulfosalicylic acid (SSA), ethylenediaminetetraacetic acid (EDTA), triton-X-100, and sodium phenylpyruvate (PhP) were obtained from Sigma Chemical Co. (St. Louis, MO). 1-Fluoro-2-4-dinitrophenyl-5-L-alanine amide (Marfey's reagent) was obtained from Pierce Chemical Co. Inc. (Rockford, IL). Hank's balanced salt solution was obtained from Gibco (Grand Island, NY). Dulbecco's modified Eagle's Medium (DMEM) (1x) with 4500 mg/L glucose, and sodium pyruvate but without L-glutamine, Met, and cystine was purchased from HyClone (Logan, UT). HPLC-grade acetonitrile was obtained from Fisher Scientific (Fair Lawn, NJ). All other chemicals and reagents were of the highest quality commercially available.

Animals. Male and female B6C3F1 mice (7-11 weeks old) were purchased from Jackson Laboratories (Bar Harbor, ME). Mice were maintained on a 12-h light/dark cycle and were allowed feed and water ad libitum. Hepatocytes were isolated at the same time of day to minimize the effects of circadian variation on GSH levels and other enzymatic activities of interest. Hepatocytes were isolated using the two-step EDTA / collagenase perfusion method as described previously (Kemper et al., 2001; Dever and Elfarra, 2008). Initial cell yield and viability were determined by TB exclusion using a hemacytometer. Only hepatocytes with an initial overall viability of greater than 85% after isolation were used in experiments. Cells were then diluted to a concentration of 1×10^6 cells / mL in DMEM and maintained on ice until use.

DMD #23390

Cell Incubations. Incubations were carried out in 24-mL vials with screw caps fitted with Teflon-faced septa. Samples of suspended hepatocytes (2.5 mL of 1×10^6 cells/mL) were transferred to the vials. Vial samples were purged with 95% O₂ / 5% CO₂ (carbogen) before incubation at 37°C with gentle shaking (140 rpm). Following a 4 min preincubation, 131.5 µL of MetO solution dissolved in DMEM was added to each 2.5 mL cell sample resulting in a final concentration of 10-30 mM MetO. For studies with AOAA, 118.4 µL of MetO solution was added followed by 13.1 µL of AOAA dissolved in DMEM resulting in a final concentration of 30 mM MetO and 0.2 mM AOAA. Samples were then repurged with carbogen and incubated for 0-5 h. Cell incubations were terminated by being placed on ice. After gentle mixing, aliquots were collected for metabolic and toxicological analysis.

Determination of Cell Viability. TB exclusion and LDH leakage were determined as previously described (Cummings et al. 2000; Dever and Elfarra, 2008).

Quantitation of GSH and GSSG. Samples were obtained to measure intracellular and medium levels of GSH and GSSG. Briefly, 500 µL of cell sample was centrifuged at 50 g for 2 min. An aliquot of the supernatant (200 µL) was then added to 800 µL of 5% SSA to be used for analysis of GSH and GSSG levels in the medium. The cell pellet was then washed with 1 mL of ice cold phosphate-buffered saline (137 mM NaCl, 10 mM phosphate, 2.7 mM KCl, pH=7.4). Following centrifugation as described above, the supernatant was removed from the pellet and 1.25 mL of 5% SSA was added. The

DMD #23390

resulting solution was transferred to a clean microcentrifuge tube and stored at -80°C until analysis. GSH and GSSG levels were measured as previously described (Tietze, 1969; Gunnarsdottir and Elfarra, 2003; Dever and Elfarra, 2006).

Analysis of Met-*d*-O, Met-*l*-O, and Met. Samples were obtained to measure intracellular levels of Met-*d*-O, Met-*l*-O and Met. Briefly, 1.8 mL of cell sample was placed in a test tube. Samples were then centrifuged at 50 *g* for 2 min to gently pellet the cells. The supernatant was removed and 10 mL of ice-cold phosphate buffered saline was added to wash the cells. Separate experiments confirmed that a total of 3 washes with 10 mL phosphate buffered saline each wash was sufficient to remove detectable extracellular MetO from the cell sample. Following removal of the final wash supernatant, cell samples were deproteinized by addition of 0.8 mL of ice-cold ethanol. The samples were then centrifuged at 3000 rpm for 10 min. The supernatant was placed in a separate tube and dried via nitrogen stream. The dried residue was then redissolved in 200 μ L deionized water and filtered with an Acrodisc LC-13 membrane filter (Pall Gelman Sciences, Ann Arbor, MI). To increase the molar absorptivity of Met and MetO and to resolve Met-*d*-O from Met-*l*-O, samples were derivatized with 1-fluoro-2-4-dinitrophenyl-5-L-alanine amide (Marfey's reagent) using an adaption of a previously described method (Marfey, 1984; Dever and Elarra, 2006). *S*-Methyl-L-cysteine (100 ppm) was used as an internal standard. Vials containing 5 μ L internal standard, 40 μ L sample, 75 μ L 0.5% Marfey's reagent (dissolved in acetone), and 15 μ L 1 M NaHCO₃ were heated at 40°C for 60 min. Following derivatization, 7.5 μ L 2 M HCl was added to each vial. The derivatized products were analyzed by HPLC with UV detection at 340 nm

DMD #23390

as described previously (Dever and Elfarra, 2006). Typical retention times for derivatized Met-*d*-O, Met-*l*-O, *S*-methyl-L-cysteine, and Met were 20.4, 21.9, 34.5, and 36.9 min, respectively. The identity of the two derivatized MetO diastereomers were determined previously (Dever and Elfarra, 2006). To quantitate Met-*d*-O, Met-*l*-O, and Met, standard curves for each metabolite were generated. The limits of quantitation were 0.6 nmol / 10⁶ cells for all three metabolites.

Analysis of MetO transamination activity. Using a method adapted from Copper and Pinto (2005), a spectrophotometric assay was developed to measure PhP consumption due to MetO transamination by GTK in mouse liver cytosol. For this assay, all solutions were made in phosphate buffer (0.1 M KH₂PO₄, 0.1 M KCl, 5 mM EDTA, pH=7.4). Briefly, 25 μL aliquots of 2.4 mM PhP, buffer or 120 mM MetO, and buffer or 0.8 mM AOAA were combined in an eppendorf. Samples were preincubated at 37°C for 4 min. Following preincubation, 25 μL of mouse liver cytosol (0.4 mg protein) was added to the mixture to start the reaction. The protein concentration of cytosol was measured as described by Lowry et al. (1951) using bovine serum albumin as the standard. Samples were incubated for 0, 10, 20, or 30 min after which 90 μL of sample was added to 0.9 mL of 3.3 N NaOH to quench the reaction. Absorbance at 322 nm was then measured. Specific activity was calculated based on the loss of PhP from 0-30 min. To calculate nmoles PhP, the extinction coefficient of PhP at 322 nm in 3 N NaOH (24,000 cm⁻¹M⁻¹) was used (Cooper, 1978).

DMD #23390

Statistics. Metabolite areas under the curve (AUC) were calculated by trapezoidal approximation using the AREA transform of the SigmaPlot software package (SPSS Inc., Chicago, IL). Statistical analyses were carried out using the SigmaStat software program (SPSS Inc., Chicago, IL). Comparisons of means were done by paired t-test or analysis of variance. Post hoc comparisons were carried out using the Student-Newman-Keul method.

DMD #23390

Results

HPLC analysis of the stock MetO used in incubations confirmed that it was a 1:1 racemic mixture of Met-*d*-O and Met-*l*-O. Male hepatocytes exposed to 20 and 30 mM MetO had decreased cell viability at 3 h as determined by TB exclusion (Figure 2A) and LDH leakage (Figure 2C) compared to control hepatocytes exposed to vehicle alone. MetO-exposed male hepatocytes also exhibited dose-dependent GSH depletion (Figure 3A) without GSSG formation at 2 h (30 mM MetO) or 3 h (20 mM MetO). Incubations with 10 mM MetO resulted in no detectable cytotoxicity or GSH depletion (data not shown). Exposure of female hepatocytes to 30 mM MetO resulted in no cytotoxicity (Figure 2B and 2D) and increased cellular GSH levels (Figure 3B) at 2 and 3 h compared to hepatocytes exposed to vehicle alone. Medium GSH levels in Met-exposed male and female hepatocytes were lower than hepatocytes exposed to vehicle alone starting at 3 h and 2 h, respectively (Figure 3C and 3D). Cellular and medium GSSG levels in MetO-exposed hepatocytes of both genders were similar to or lower than levels in hepatocytes exposed to vehicle alone (data not shown).

To characterize MetO uptake and metabolism to Met, a sensitive HPLC method (Figure 4) was developed to simultaneously detect and quantitate Met-*d*-O, Met-*l*-O and Met levels in male and female hepatocytes exposed to 30 mM MetO or vehicle alone at 0, 0.5, 1, and 1.5 h (Figure 5). These data were also used to calculate AUC for cellular MetO concentration versus time ($AUC_{0-1.5\text{ h}}$). The results are presented in Table 1. Total MetO levels were approximately 2-fold higher at 0.5 and 1 h, and 1.3-fold higher at 1.5 h in MetO-exposed male hepatocytes compared to MetO-exposed female hepatocytes (Figure 5A and 5B) resulting in a significantly higher $AUC_{0-1.5\text{ h}}$ (Table 1). MetO-

DMD #23390

exposed male hepatocytes had Met-*d*-O and Met-*l*-O AUC_{0-1.5 h} values that were nearly 2-fold higher than values in MetO-exposed female hepatocytes. Male hepatocytes exposed to vehicle alone also had significantly higher cellular levels of total MetO compared to females where very little endogenous MetO was detected. In MetO-exposed hepatocytes of both genders, Met-*l*-O was the primary diastereomer detected (80-85%) at all time points, and no significant increases in Met levels were detected relative to controls.

To assess the role of MetO TA in MetO metabolism and toxicity in male mouse hepatocytes, the effects of the transaminase inhibitor AOAA were investigated. Addition of AOAA (0.2 mM) reduced MetO-induced GSH depletion and cytotoxicity compared to hepatocytes exposed to 30 mM MetO alone (Figure 6). No effect on cellular GSH levels or viability was detected in control male hepatocytes incubated with only AOAA (data not shown). Addition of AOAA (0.2 mM) increased Met-*d*-O levels at 0.5 and 1.5 h and increased Met-*l*-O levels at 1.5 h in MetO-exposed male hepatocytes compared to hepatocytes exposed to only MetO (Figure 7A and 7B). The AOAA treatment did not lead to any changes in Met levels in MetO or vehicle treated hepatocytes. Interestingly, exposure of control male hepatocytes exposed to only AOAA resulted in significant increases in cellular Met-*d*-O levels starting at 1 h (Figure 7C) without any detectable increases in cellular Met-*l*-O (Figure 7D) or Met levels. The levels of Met-*d*-O detected in control male hepatocytes in the presence of AOAA were similar to the levels detected in hepatocytes exposed to 30 mM MetO.

Since MetO TA appeared to play a significant role in MetO metabolism and toxicity, an assay was developed to measure MetO transamination activity by GTK in male and female mouse liver cytosol as a function of MetO-induced depletion of PhP, an

DMD #23390

amino acceptor substrate for GTK with strong absorbance at 322 nm. Linear depletion of PhP from 0-30 min was detected in male and female cytosol incubated with MetO (30 mM), (Figure 8A and 8B) resulting in a similar specific activity for PhP depletion due to MetO transamination (8C) in cytosolic samples of both genders. Addition of AOAA resulted in nearly complete inhibition of PhP depletion in cytosol of both genders incubated with MetO. No significant PhP depletion was detected in male or female cytosol incubated without MetO.

DMD #23390

Discussion

Cytotoxicity and GSH depletion without formation of GSSG were detected in male hepatocytes incubated with 20 or 30 mM MetO. MetO-exposed male hepatocytes incubated with AOAA were significantly protected from both MetO-induced cytotoxicity and GSH depletion indicating that TA plays a major role in eliciting MetO toxicity. Further support for this hypothesis is provided by the finding that cellular levels of both MetO diastereomers were 1.5- to 2-fold higher at 1.5 h in male hepatocytes exposed to MetO and AOAA compared with hepatocytes exposed to only MetO.

That MetO toxicity resulted in GSH depletion without GSSG formation implies that MetO TA leads to the formation of GSH-reactive metabolites. Transamination of MetO is expected to result in formation of 2-keto-4-(methylsulfinyl)butyric acid, the analog of 2-keto-4-(methylthio)butyric acid, the keto-acid formed from Met TA. 2-Keto-4-(methylthio)butyric acid is known to be oxidatively decarboxylated to 3-methylthiopropionic acid (Steele and Benevenga, 1978; Jones and Yeaman, 1986) which is further metabolized to methanethiol, a metabolite that has been shown to react with sulfhydryl groups to form protein and non-protein mixed disulfides and inhibit enzyme activity (Steele and Benevenga, 1979; Finkelstein and Benevenga, 1986; Blom et al., 1988; Gahl et al., 1988; Tangermen et al., 2000). Similar metabolism of 2-keto-4-(methylsulfinyl)butyric acid would result in formation of methanesulfenic acid which could also react with sulfhydryl groups to form mixed disulfides (Rose et al., 2005). Thus, formation of methanesulfenic acid could play a significant role in the mechanism by which MetO causes GSH depletion and cytotoxicity.

DMD #23390

In comparison to male hepatocytes, female hepatocytes were completely resistant to MetO cytotoxicity and actually had higher cellular GSH levels at 2 and 3 h compared to hepatocytes exposed to vehicle only. At these same time points, GSH levels in the medium of MetO-exposed female hepatocytes were lower compared to hepatocytes exposed to vehicle only. A similar effect was previously noted in female hepatocytes incubated with Met (Dever and Elfarra, 2008) and may be due to inhibition of cellular GSH efflux by Met (Aw et al., 1986).

To further investigate the underlying mechanisms of Gender differences in MetO toxicity and to investigate potential cellular accumulation of Met after MetO exposure, cellular MetO and Met levels were quantitated and compared in MetO-exposed male and female hepatocytes. The time range for these metabolic analysis (0-1.5 h) was chosen because it preceded MetO-induced GSH depletion in males at 2 h. For both male and female hepatocytes, the maximum intracellular MetO levels detected were less than 1% of the total MetO present in medium indicating that a significant depletion of media MetO concentrations did not occur.

Total cellular MetO levels at 0.5 h and 1 h in MetO-exposed female hepatocytes were approximately half of those in males. Additionally, by employing a convenient spectrophotometric assay, MetO transamination activity by GTK measured in mouse liver cytosol revealed similar rates of MetO transamination in cytosolic samples of both genders. While other transaminases may also be involved in MetO transamination, these results provided evidence that gender differences in MetO toxicity are not due to differences in MetO transamination activity. Taken together, these data suggest that a

DMD #23390

lower rate of cellular MetO uptake is the most likely explanation for the insensitivity of female hepatocytes to MetO toxicity.

Despite the detection of significant gender differences in cellular MetO levels in MetO-exposed hepatocytes, Met-*l*-O was the major MetO diastereomer detected (80-85% of total MetO) in MetO-exposed hepatocytes of both genders at all time points. Since hepatocytes were exposed to racemic MetO, this suggests the preferential uptake of Met-*l*-O and/or preferential metabolism of Met-*d*-O in both males and females.

Stereoselective reduction of MetO is known to be carried out by MsrA, which selectively reduces Met-*d*-O (also referred to as Met-*S*-O) or MsrB which selectively reduces Met-*l*-O (also referred to as Met-*R*-O) (Moskovitz et al., 2000; Moskovitz et al., 2002). In *E. Coli*, the catalytic efficiency (K_{cat}/K_m) of MsrA reduction of free Met-*d*-O was 1000-fold greater than MsrB reduction of free Met-*l*-O (Grimaud et al., 2001) indicating that cellular Met-*d*-O may be more readily reduced than Met-*l*-O. Indeed, reduction of Met-*d*-O (1 mM) in mouse liver and kidney homogenates proceeded with a 1.2-fold and 2-fold higher specific activity, respectively, than reduction of Met-*l*-O (Moskovitz et al., 2002). Thus, increased reduction of Met-*d*-O compared to Met-*l*-O could explain the detection of mostly Met-*l*-O in hepatocytes upon exposure to racemic MetO. While no increase in Met formation was detected in hepatocytes with high intracellular levels of MetO, stereoselective reduction of MetO cannot be ruled out since it is possible that Met formed from MetO reduction was rapidly utilized and, consequently, not detected.

In male hepatocytes, AOAA increased cellular levels of both Met-*d*-O and Met-*l*-O levels. These results suggest that the TA reaction of MetO is not selective for one of the two diastereomers. Interestingly, however, an unexpected increase in Met-*d*-O levels

DMD #23390

was detected in control male mouse hepatocytes exposed to AOAA suggesting that formation and subsequent transamination of Met-*d*-O may occur under normal physiological conditions. Consistent with this finding, low levels of mostly Met-*d*-O were previously detected in the livers of control male and female mice whereas in Met-dosed mice, higher levels of Met-*d*-O were present in liver (Dever and Elfarra, 2006). Taken together, these results provide evidence for enzymatic Met-*d*-O formation, but additional studies are necessary to further characterize the Met S-oxidase activities in male mouse liver.

Several conclusions can be drawn regarding the potential role of Met S-oxidation in Met metabolism and toxicity. Because MetO toxicity was elicited at similar concentrations as Met toxicity in male hepatocytes (Dever and Elfarra, 2008), MetO formation does not represent a clear bioactivation or detoxification pathway for Met. It is also unlikely that the MetO concentrations required to elicit toxicity (20 mM) in male hepatocytes in this study would be achieved *in vivo*. Thus, we conclude that the role of Met S-oxidation in Met toxicity is merely additive to that of the toxic Met TA metabolites.

The significant buildup of Met-*d*-O in control male hepatocytes exposed to AOAA suggests Met-*d*-O formation is a significant pathway of Met metabolism under physiological conditions and that MetO TA plays a significant role in the metabolism of Met-*d*-O. Currently, there is no information regarding the metabolic fate of 2-keto-4-(methylsulfinyl)butyric acid. Further studies will be necessary to fully assess the role of MetO TA in cellular metabolism. Additionally, the finding that similar Met-*d*-O levels were detectable in control and MetO-treated hepatocytes in the presence of AOAA

DMD #23390

suggests the presence of an alternative pathway for Met-*d*-O metabolism once it reaches the levels observed in control and MetO-treated hepatocytes exposed to AOAA.

In summary, MetO toxicity and several aspects of MetO metabolism have been characterized in male and female mouse hepatocytes. MetO cytotoxicity and GSH depletion were mediated by MetO TA and were gender-dependent. Accumulation of Met in MetO-exposed hepatocytes was not detected while addition of AOAA increased Met-*d*-O and Met-*l*-O levels in MetO-exposed male hepatocytes and increased Met-*d*-O levels in control male hepatocytes. Taken together, these results suggest that MetO TA plays an important role in the metabolism of MetO and that formation of Met-*d*-O after Met exposure may be enzymatically catalyzed.

DMD #23390

References

- Anderson GH, Ashley DVM and Jones JD (1976) Utilization of L-methionine sulphoxide, L-methionine sulphone, and cysteic acid by the weanling rat. *J Nutr* **106**: 1108-1114.
- Aw TY, Ookhtens M and Kaplowitz N (1986) Mechanism of inhibition of glutathione efflux by methionine from isolated rat hepatocytes. *Am J Physiol* **251**: G354-G361.
- Blom HJ, van den Elzen JP, Yap SH and Tangerman A (1988) Methanethiol and dimethylsulfide formation from 3-methylthiopropionate in human and rat hepatocytes. *Biochim Biophys Acta* **972**: 131-136.
- Cooper AJL and Meister A (1972) Isolation and properties of highly purified glutamine transaminase. *Biochemistry* **11**: 661-671.
- Cooper AJL (1978) Purification of soluble and mitochondrial glutamine transaminase K from rat kidney. *Anal Biochem* **89**: 451-460.
- Cooper AJL and Pinto JT (2005) Aminotransferase, L-amino acid oxidase and β -lyase reactions involving L-cysteine S-conjugates found in allium extracts: Relevance to biological activity. *Biochem Pharmacol* **69**: 209-220.
- Cummings BS, Zangar RC, Novak RF and Lash LH (2000) Cytotoxicity of trichloroethylene and S-(1, 2-dichlorovinyl)-L-cysteine in primary cultures of rat renal proximal tubular and distal tubular cells. *Toxicology* **150**: 83-98.
- Dever JT and Elfarra AA (2006) In vivo metabolism of L-methionine in mice: Evidence for stereoselective formation of methionine-d-sulfoxide and quantitation of other major metabolites. *Drug Metab Dispos* **34**: 2036-2043.

DMD #23390

- Dever JT and Elfarra AA (2008) L-methionine toxicity in freshly isolated mouse hepatocytes is gender-dependent and mediated in part by transamination. *J Pharmacol Exp Ther* (in press).
- Duescher RJ, Lawton MP, Philpot RM and Elfarra AA (1994) Flavin-containing monooxygenase (FMO)-dependent metabolism of methionine and evidence for FMO3 being the major FMO involved in methionine sulfoxidation in rabbit liver and kidney microsomes. *J Biol Chem* **269**: 17525-17530.
- Finkelstein A and Benevenga NJ (1986) The effect of methanethiol and methionine toxicity on the activities of cytochrome c oxidase and enzymes involved in protection from peroxidative damage. *J Nutr* **116**: 204-215.
- Gahl WA, Bernardini I, Finkelstein JD, Tangerman A, Martin JJ, Blom HJ, Mullen KD and Mudd SH (1988) Transsulfuration in an adult with hepatic methionine adenosyltransferase deficiency. *J Clin Invest* **81**: 390-397.
- Grimaud R, Ezraty B, Mitchell JK, Lafitte D, Briand C, Derrick PJ and Barras F (2001) Repair of oxidized proteins. *J Biol Chem* **276**: 48915-48920.
- Gunnarsdottir S and Elfarra AA (2003) Distinct tissue distribution of metabolites of the novel glutathione-activated thiopurine prodrugs cis-6-(2-acetylvinylthio)purine and trans-6-(2-acetylvinylthio)guanine and 6-thioguanine in the mouse. *Drug Metab Dispos* **31**: 718-726.
- Jones SMA and Yeaman SJ (1986) Oxidative decarboxylation of 4-methylthio-2-oxobutyrate by branched-chain 2-oxo acid dehydrogenase complex. *Biochem J* **237**: 621-623.

DMD #23390

- Kemper RA, Krause RJ and Elfarra AA (2001) Metabolism of butadiene monoxide by freshly isolated hepatocytes from mice and rats: Different partitioning between oxidative, hydrolytic, and conjugation pathways. *Drug Metab Dispos* **29**: 830-836.
- Lowry OH, Rosebrough NJ, Farr AL, and Randall RJ (1951) Protein measurement with the folin phenol reagent. *J Biol Chem* **193**: 265-275.
- Marfey P (1984) Determination of D-amino acids. II. Use of a bifunctional reagent, 1,5-difluoro-2,4-dinitrobenzene. *Carlsburg Res Commun* **49**: 591-596.
- Mashima R, Nakanishi-Ueda T and Yamamoto Y (2003) Simultaneous determination of methionine sulphoxide and methionine in blood plasma using gas chromatography-mass spectrometry. *Anal Biochem* **313**: 28-33.
- Miller SA, Tannenbaum SR and Seitz AW (1970) Utilization of L-methionine sulfoxide by the rat. *J Nutr* **100**: 909-916.
- Mitchell AD and Benevenga NJ (1978) The role of transamination in methionine oxidation in the rat. *J Nutr* **108**: 67-78.
- Moskovitz J, Poston JM, Berlett BS, Nosworthy NJ, Szczepanowski R and Stadtman ER (2000) Identification and characterization of a putative active site for peptide methionine sulphoxide reductase (MsrA) and its substrate stereospecificity. *J Biol Chem* **275**: 14167-14172.
- Moskovitz J, Singh VK, Requena J, Wilkinson BJ, Jayaswal RK and Stadtman ER (2002) Purification and characterization of methionine sulfoxide reductases from mouse and staphylococcus aureus and their substrate stereospecificity. *Biochem Biophys Res Commun* **290**: 62-65.

DMD #23390

Moss LR, Haynes AL, Pastuszyn A and Glew RH (1999) Methionine infusion reproduces liver injury of parenteral nutrition cholestasis. *Pediatr Res* **45**: 664-668.

Perry TL, Hansen S and MacDougall L (1967) Sulfur-containing amino acids in plasma and urine of homocystinurics. *Clin Chim Acta* **15**: 409-420.

Ripp SL, Kiyoshi I, Philpot RM and Elfarra AA (1999) Species and sex differences in expression of flavin-containing monooxygenase form 3 in liver and kidney microsomes. *Drug Metab Dispos* **27**: 46-52.

Rose P, Whiteman M, Moore P and Zhu YZ (2005) Bioactive S-alk(en)yl cysteine sulphoxide metabolites in the genus *Allium*: the chemistry of potential therapeutic agents. *Nat Prod Rep* **22**: 351-368.

Sharov VS and Schoneich C (2000) Diastereoselective protein methionine oxidation by reactive oxygen species and diastereoselective repair by methionine sulfoxide reductase. *Free Rad Biol Med* **29**: 986-994.

Shinozuka H, Estes LW and Farber E (1971) Studies on acute methionine toxicity. I. Nucleolar disaggregation in guinea pig hepatic cells with methionine or ethionine and its reversal with adenine. *Amer J Path* **64**: 241-249.

Smith RC (1972) Acetylation of methionine sulfoxide and methionine sulfone by the rat. *Biochim Biophys Acta* **261**: 304-309.

Stadtman ER, Remmen HV, Richardson A, Wehr NB and Levine RL (2004) Methionine oxidation and aging. *Biochim Biophys Acta* **1703**: 135-140.

Steele RD, Barber TA, Lalich J and Benevenga NJ (1978) Effects of dietary 3-methylthiopropionate on metabolism, growth, and hematopoiesis in the rat. *J Nutr* **109**: 1739-1751.

DMD #23390

Steele RD and Benevenga NJ (1978) Identification of 3-methylthiopropionic acid as an intermediate in mammalian methionine metabolism in vitro. *J Biol Chem* **253**: 7844-7850.

Steele RD and Benevenga NJ (1979) The metabolism of 3-methylthiopropionate in rat liver homogenates. *J Biol Chem* **254**: 8885-8890.

Stegink LD, Bell EF, Filer LJ, Ziegler EE, Anderson DW and Seligson FH (1986) Effects of equimolar doses of L-methionine, D-methionine and L-methionine-*dl*-sulfoxide on plasma and urinary amino acid levels in normal adults humans. *J Nutr* **116**: 1185-1192.

Tangerman A, Wilcken B, Levy HL, Boers GHJ and Mudd SH (2000) Methionine transamination in patients With homocystinuria due to cystathionine β -synthase deficiency. *Metabolism* **49**: 1071-1077.

Tietze F (1969) Enzymatic method for quantitative determination of nanogram amounts of total and oxidized glutathione: applications to mammalian blood and other tissues. *Anal Biochem* **27**: 502-522.

DMD #23390

Footnotes

This research is supported by NIH R01 DK044295 and T32-ES-007015.

Corresponding author:

Dr. Adnan Elfarrar
University of Wisconsin
School of Veterinary Medicine
2015 Linden Drive
Madison, WI 53706-1102
(608)262-6518 - office
(608)263-3926 – fax
elfarra@svm.vetmed.wisc.edu

DMD #23390

Figure Legends

Figure 1. Schematic of potential MetO metabolic pathways. Bolded metabolites have been previously detected *in vivo* in rats fed excess MetO.

Figure 2. Time course of the cell viability of male (n=4) or female (n=3) hepatocytes exposed to vehicle alone or MetO as determined by TB exclusion (A, B) and LDH leakage (C, D). The symbol * indicates values that were significantly lower than hepatocytes incubated with vehicle alone (*p<0.05). Data are expressed as mean ± SD.

Figure 3. Time course of intracellular (A, B) and medium (C, D) GSH levels of male (n=7 for 20 mM and n=4 for 30 mM) or female (n=3) hepatocytes exposed to vehicle alone or MetO. The symbol * indicates values that were significantly different than hepatocytes incubated with vehicle alone (*p<0.05). Data are expressed as mean ± SD.

Figure 4. Representative chromatograph of Met-*d*-O, Met-*l*-O, and Met in male mouse hepatocytes after incubation with 30 mM MetO or vehicle alone for 90 min. 1=Met-*d*-O, 2=Met-*l*-O, 3=S-methyl-L-cysteine (internal standard), 4=Met. The identities of the peaks at 35.2, 35.8 min were not determined.

Figure 5. Time course of total MetO (A, B) and Met (C, D) levels in male (n=4) or female (n=3) hepatocytes exposed to vehicle alone or 30 mM MetO. The symbol *

DMD #23390

indicates values that were significantly higher than hepatocytes incubated with vehicle alone (* $p < 0.05$). Data are expressed as mean \pm SD.

Figure 6. Time course of TB exclusion viability (A), LDH leakage viability (B), and intracellular GSH levels (C) of male hepatocytes (n=4) exposed to vehicle alone, 30 mM MetO, or 30 mM MetO and 0.2 mM AOAA. The symbol * indicates values that were significantly lower than cells incubated with vehicle alone ($p < 0.05$). The symbol † indicates values that were significantly higher than hepatocytes incubated with 30 mM MetO ($p < 0.05$). Data are expressed as mean \pm SD.

Figure 7. Time course of the effect of AOAA on cellular Met-*d*-O (A, C) and Met-*l*-O (B, D) levels in male hepatocytes (n=3) exposed to 30 mM MetO (A, B), or vehicle alone (C, D). The symbol * indicates values that were significantly higher than hepatocytes incubated without AOAA (* $p < 0.05$). Data are expressed as mean \pm SD.

Figure 8. Time course of PhP (0.6 mM) depletion in male (n=4) or female (n=3) cytosol (A, B) after incubations at 37°C with vehicle alone, 30 mM MetO, or 30 mM MetO and 0.2 mM AOAA. These time course data were then used to calculate specific activity of MetO-induced PhP depletion in each gender (C). Data are expressed as mean \pm SD.

DMD #23390

Table 1. Area Under the Curve (AUC) analysis for Met-*d*-O, Met-*l*-O, total MetO, and Met in male and female hepatocytes exposed to 30 mM Met-*dl*-O or vehicle alone.

Treatment	AUC _{0-1.5h} (nmol · h / 10 ⁶ cells)			
	Met- <i>d</i> -O	Met- <i>l</i> -O	MetO (total)	Met
30 mM Met- <i>dl</i> -O				
Male	11.8±0.9 ^{ab}	59.6±12.3 ^b	71.7±12.7 ^b	1.2±0.6
Female	6.9±3.5	32.0±13.8	38.8±17.4	1.0±0.5
Vehicle alone				
Male	2.0±0.7 ^b	5.9±3.7	7.8±4.4 ^b	0.7±0.8
Female	0.0±0.0	0.4±0.7	0.4±0.7	0.8±0.9

^a Data are expressed as mean ± SD (n = 3-4).

^b indicates values that were significantly higher than the corresponding values obtained with the opposite sex.

Figure 1

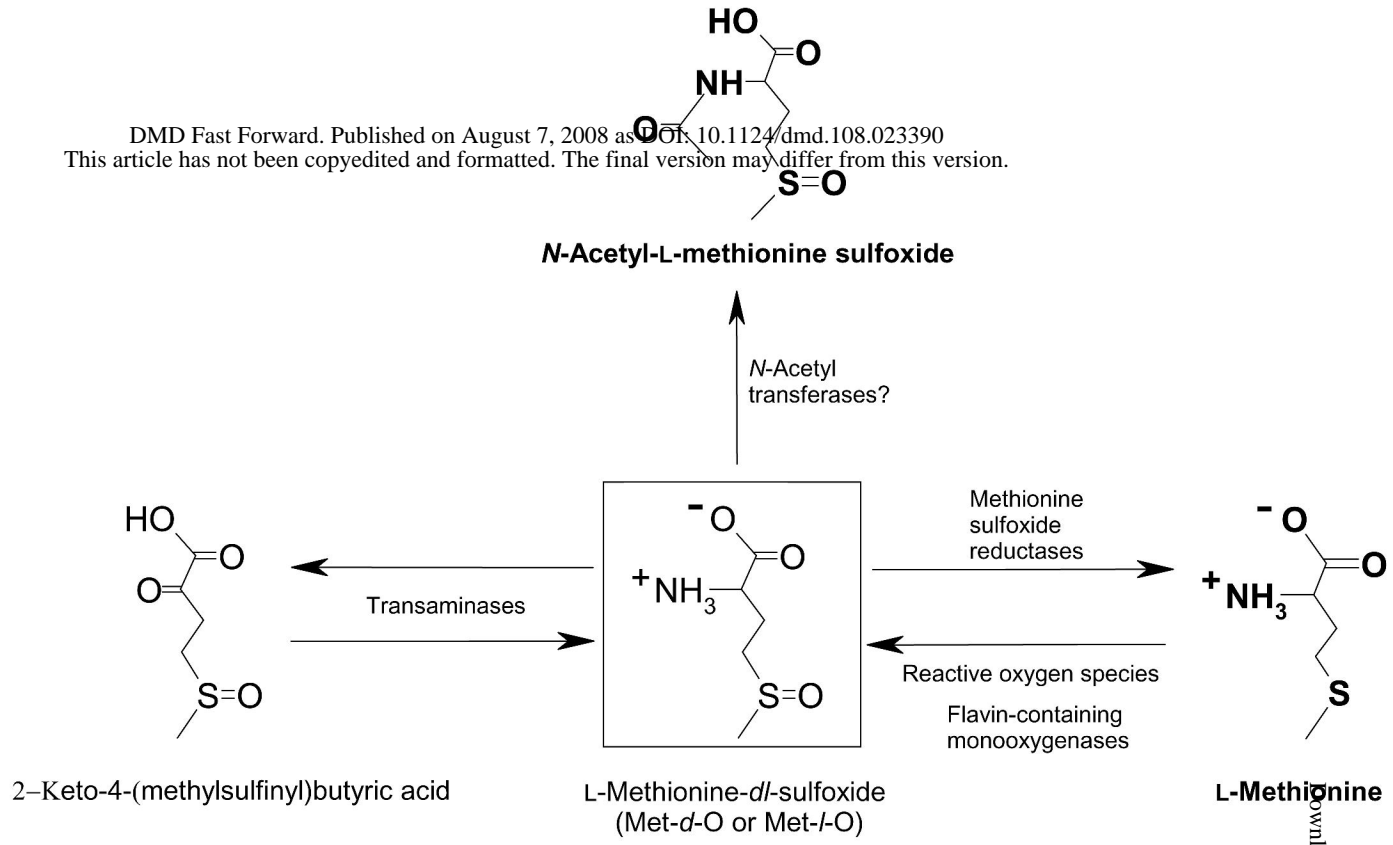
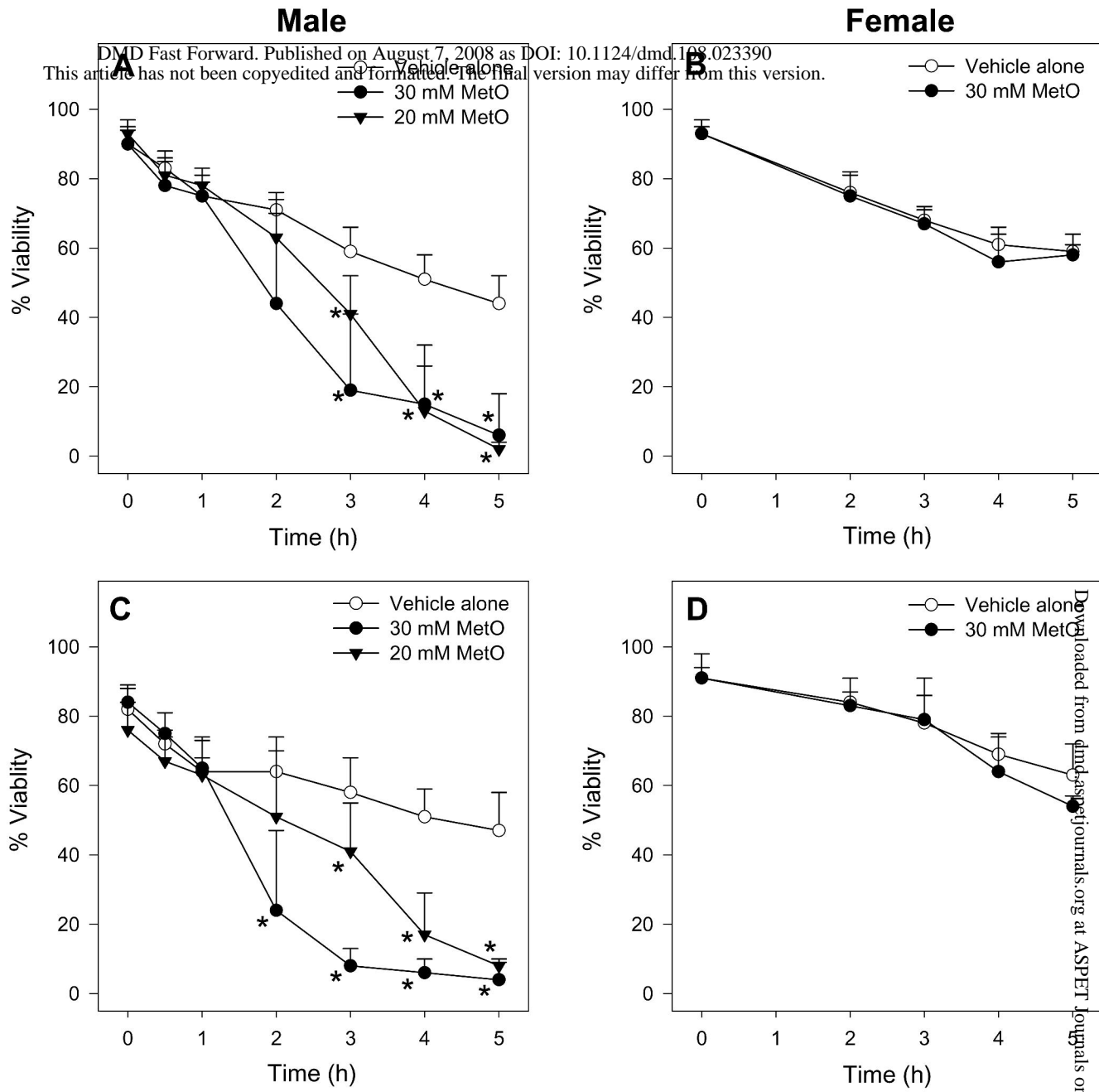


Figure 2



Downloaded from dmd.aspetjournals.org at ASPET Journals on April 19, 2024

Figure 3

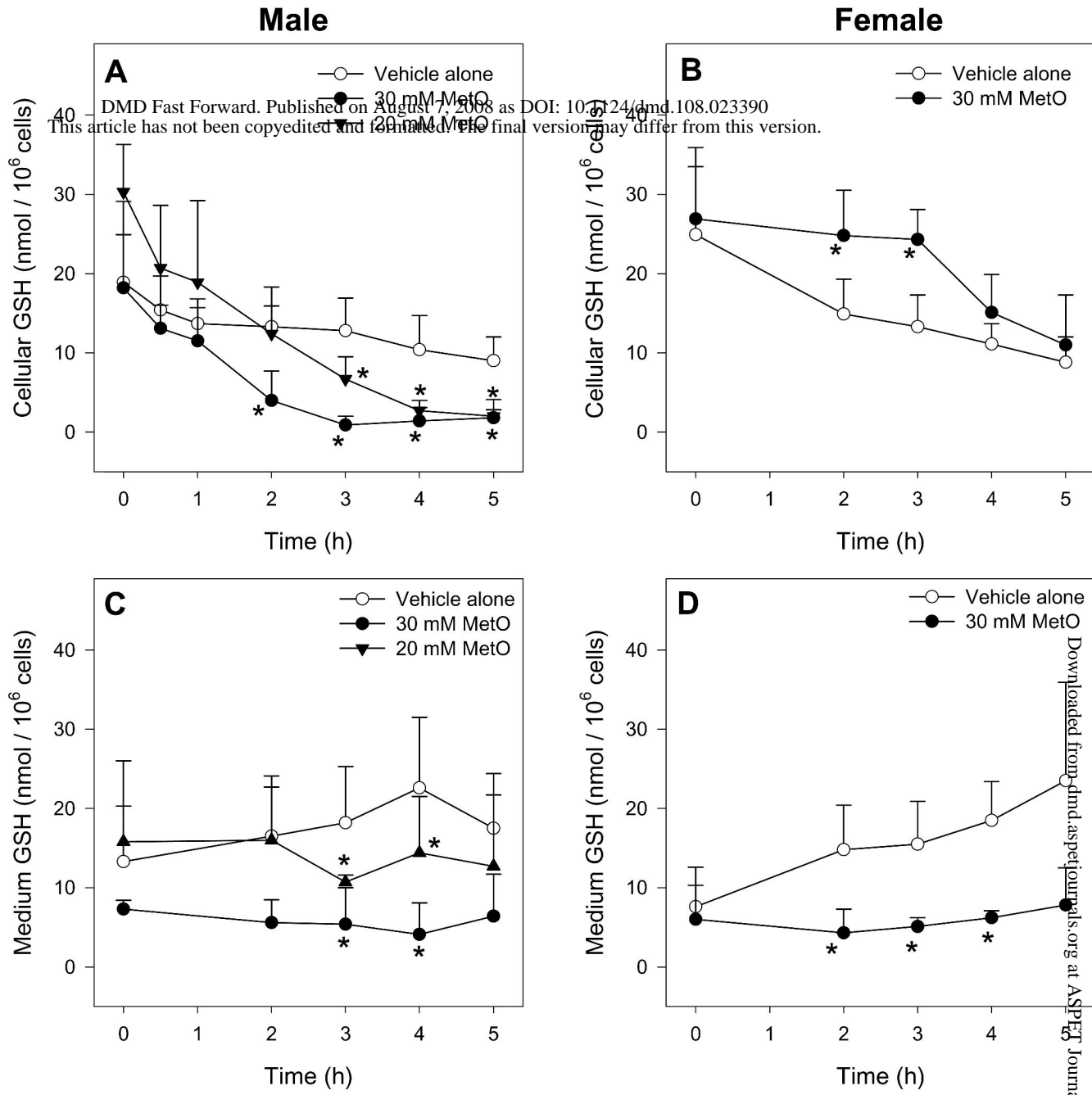
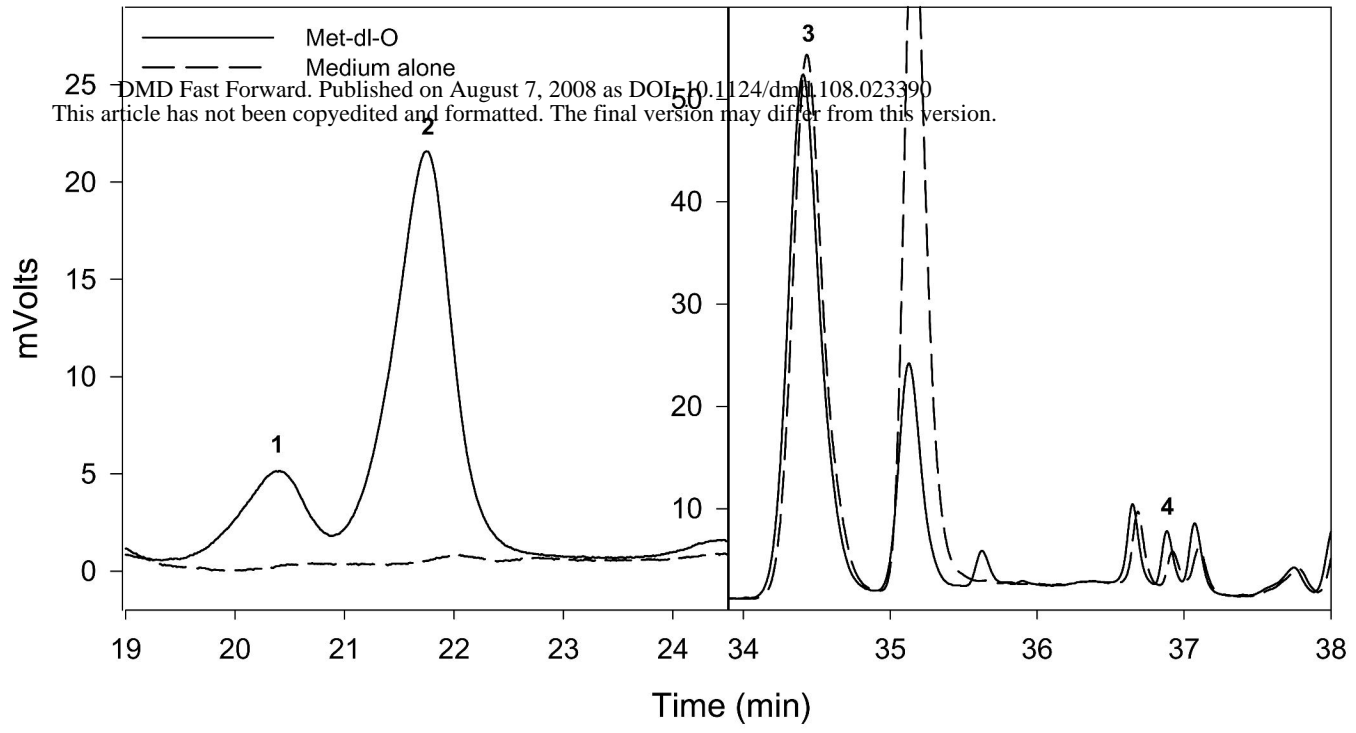
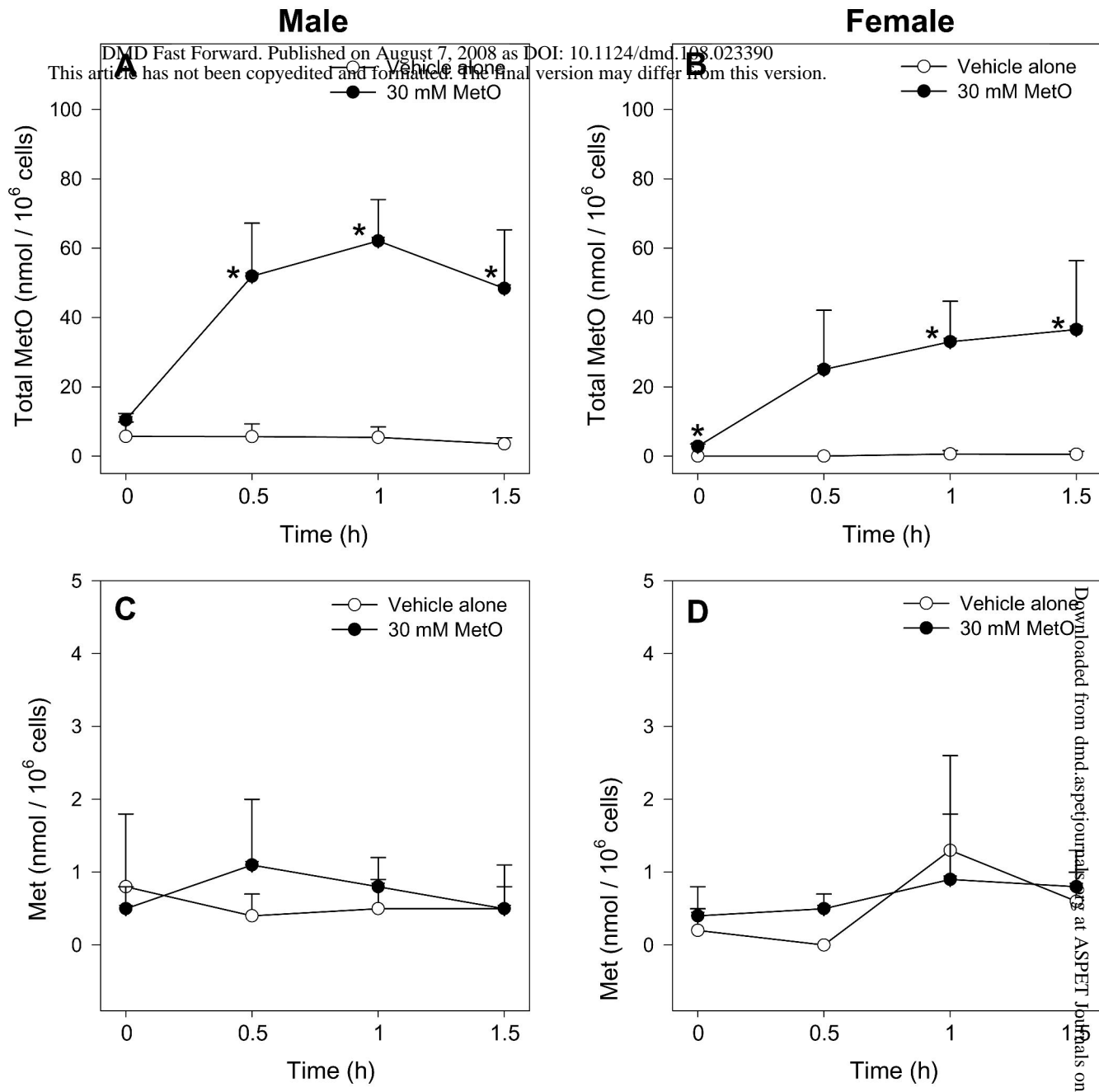


Figure 4



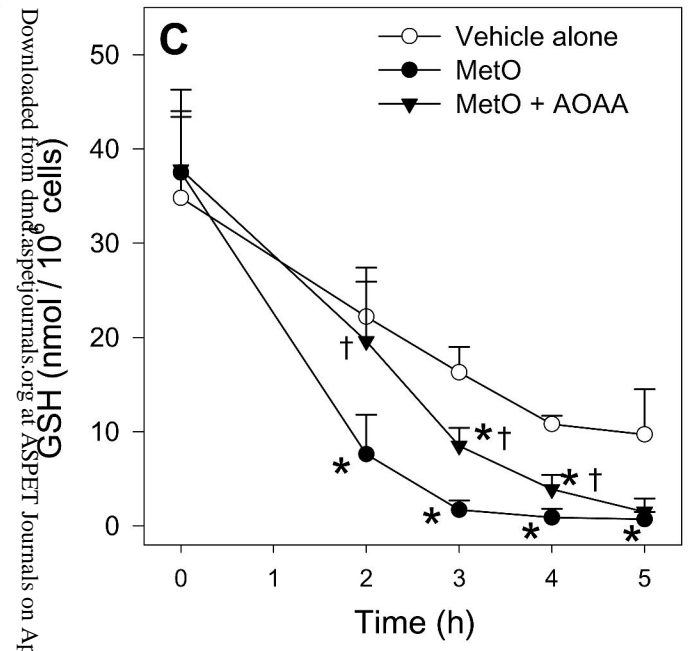
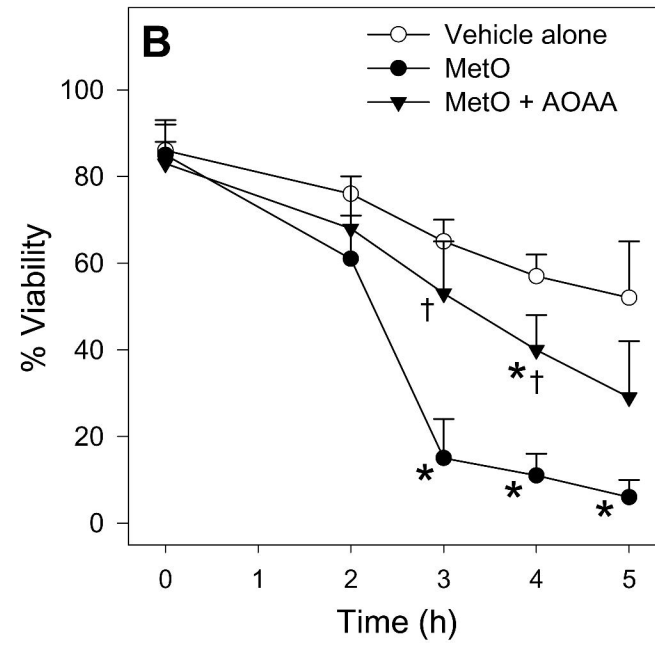
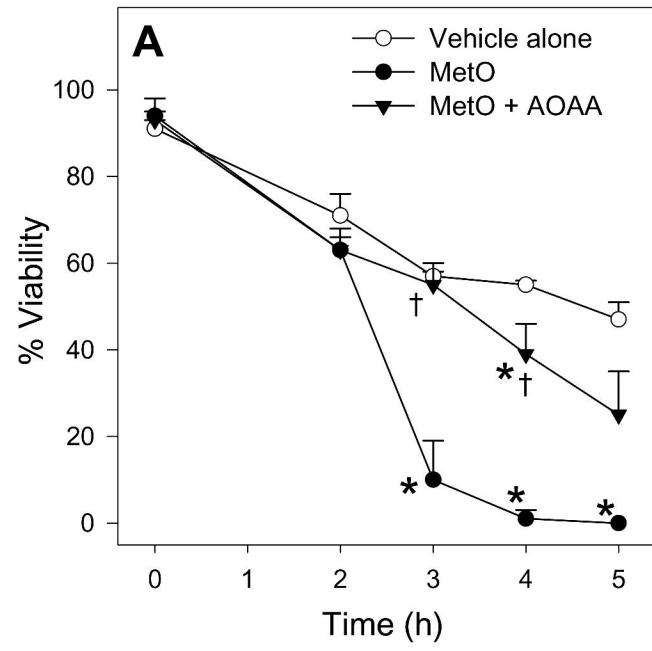
25 DMD Fast Forward. Published on August 7, 2008 as DOI: 10.1124/dmd.108.023390
This article has not been copyedited and formatted. The final version may differ from this version.

Figure 5



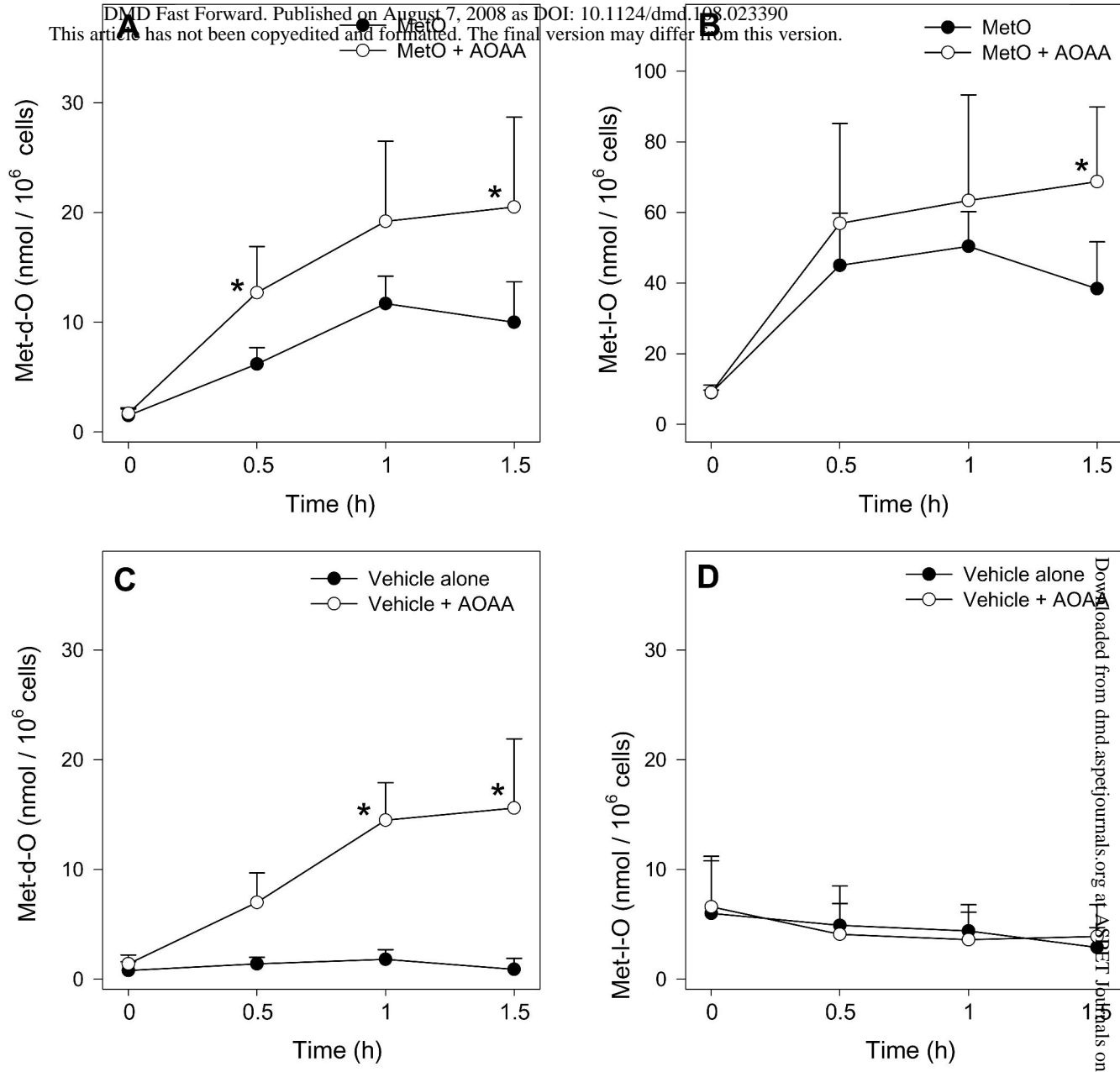
Downloaded from dmd.aspetjournal.org at ASPET Journals on April 19, 2024

Figure 6



Downloaded from dndi.aspenjournals.org at ASPET Journals on April 19, 2024

Figure 7



Downloaded from dmd.aspetjournals.org at ASPET Journals on April 19, 2024

Figure 8

